

# ANALYSIS OF OPTIMAL WIND POWER INTEGRATION CAPACITY BASED ON THE SCENARIO TREE CONSTRUCTION METHOD

*Yingzhao Xie, Jiping Lu*

Original scientific paper

The determination of the optimal wind power integration capacity of a large-scale wind farm has become an important issue in power system operation and planning. Reasonable wind power integration capacity can improve the wind energy utilization and save investment for wind farm construction. This paper builds a mathematical model for determining wind farm optimal integration capacity by taking the maximization of the wind farm annual generation net benefits the objective function and the security operation requirements as the model constraints. The scenario tree construction method is proposed to deal with the random characteristics of wind power in one year based on the probability theory. The discretization principles of wind speed probability distribution and the scenario tree construction processes of wind power are proposed. Hierarchical optimization algorithm combining w-particle swarm optimization algorithm and social emotional optimization algorithm is used to solve the optimization model in this paper. The effects caused by the variation of factors correlated with the optimal wind power integration capacity results are investigated using the proposed model. The detailed solution steps are given. The correctness of the model and the validity of the algorithms for solving are verified according to the simulation on the IEEE-30 nodes system.

**Keywords:** generation net benefit, optimal integration capacity, scenario tree construction method, social emotional optimization algorithm, wind farm

## Analiza optimalnog integrativnog kapaciteta energije vjetra na temelju metode konstrukcije stabla scenarija

Izvorni znanstveni članak

Određivanje optimalnog integrativnog kapaciteta energije vjetra velike vjetroelektrane postalo je važno pitanje kod planiranja i rada energetskog postrojenja. Razumni integrativni kapacitet energije vjetra može poboljšati korištenje energije vjetra i uštedjeti na ulaganju za izgradnju vjetroelektrane. U ovom je radu prikazan matematički model za određivanje optimalnog integrativnog kapaciteta vjetroelektrane uzimajući maksimalizaciju čiste dobiti godišnje proizvodnje vjetroelektrane kao objektivnu funkciju, a potrebe osiguranja kao ograničenja modela. Metoda konstrukcije stabla scenarija predložena je zbog bavljenja nesistematskim karakteristikama energije vjetra tijekom jedne godine na temelju teorije vjerojatnosti. Predloženi su principi diskretizacije vjerojatnoće raspodjele brzine vjetra i postupci konstrukcije stabla scenarija energije vjetra. Primijenjen je algoritam hijerarhijske optimalizacije koji kombinira algoritam optimalizacije roja w-čestica i algoritam društveno emocionalne optimalizacije za rješenje modela optimalizacije u ovom radu. Predloženi se model primijenio u istraživanju učinaka izazvanih varijacijom faktora povezanih s rezultatima optimalnog integrativnog kapaciteta energije vjetra. Daju se detaljni postupci u dobivanju rješenja. Točnost modela i valjanost algoritama verificirani su prema simulaciji na sustavu IEEE-30 čvorova.

**Ključne riječi:** algoritam društveno emocionalne optimalizacije, čista dobit proizvodnje, metoda konstrukcije stabla scenarija, optimalni integrativni kapacitet, vjetroelektrana

## 1 Introduction

Wind energy is considered a renewable energy that can be utilized effectively [1 ÷ 6]. Wind energy generation technology is also the most feasible technology among the renewable energy generation technologies at present. The large-scale exploitation of wind energy has increasingly played an important role in relieving the energy crisis and protecting the environment, and has aroused the attention of most governments in the world. However, the large generation capacity and randomness of the form of wind energy generation bring new challenges to the plan and design of a power system as well as to its secure and stable operation. Therefore, the main problem that needs to be solved in the planning stage of wind farm construction is determining the optimum installation capacity of the wind farm to acquire maximum economic benefit under the premise of minimum investment cost and the guarantee of secure and stable operation of a power system.

Several influencing factors affect the determination of the installation capacity of a wind farm. The technological factors include the operation modes of wind farm along with the power system, the configuration of the power grid, and the regulation capability of the conventional generators in the power system. The economic factors include the online electricity price of wind power,

investment cost of wind farm construction, and so on. Although many scholars in different countries have conducted many studies about this problem, no universal method has been proposed for the determination of wind power integration capacity. The main analysis methods proposed for the problem at present involve simulation analysis and optimization theory. Although simulation analysis can simulate power system variation, several influencing factors on the determination of wind farm integration capacity (WFIC) make the computation complexity unacceptable and unable to reveal the regularity of the modification to the variation by adopting the simulation method. Furthermore, one simulation process usually highlights some influencing factors that are interesting to researchers and ignores the other factors [7, 8]. One process cannot simultaneously consider all the effects caused by the main factors, such as the variation of power system operation mode, the variation of wind speed condition, and so on.

Scholars have created WFIC mathematical models and provided corresponding solutions to different models according to the idea of the optimization theory to better describe and analyze the WFIC problem. The optimization method is a practical methodology that can comprehensively consider several influencing factors that affect wind farm integration capacity, such as operation mode, grid configuration, output capability of the

generator units, and correlative economic conditions. Approximate linear programming has been applied to linearize the non-linear objective function of the wind farm integration capacity model, and the solution of the approximate model has been applied to approach the exact solution of the original model [9]. An entire wind power integration capacity limit model has been created with an AC equation constraint condition. The non-linear primal-dual path tracking interior point algorithm is employed to solve this model to reduce the error caused by model linearization [10]. These optimization models focus on model simplification and solution algorithm, and equate actual output power with the rated power of the wind power generators, which belong to the certainty optimization category [9 ÷ 12]. Lei and Wu establish chance constrained programming models based on stochastic programming theory using the probability density function (PDF) to describe the randomness of wind speed and provide the probability form of the operation constraint conditions and output power limits of conventional generators to avoid conservative calculation results due to the disregard for wind speed randomness [13, 14]. Qiao and Wang analyze the effect brought by the wind farm output power reduction measure and the variation of wind turbine generator system parameters and power system operation parameters based on the solution of the stochastic optimization model [15, 16]. The original stochastic optimization model is converted to the disturbing boundary function form of random variables using robust optimization theory, which makes the original model an ordinary linear programming model format and realizes the solution of the original model [17]. Optimization models with the objective functions of maximizing wind farm economic benefits considering the power system operation constraints and the economic influencing factors are proposed [18, 19]. These optimization models consider the effect of wind speed randomness and apply different methods to describe random variables in which the Monte Carlo simulation is a common algorithm. However, using the Monte Carlo method to simulate a random process requires many calculations [13 ÷ 19]. In addition, the impact of grid location of wind farms on economic and operational parameters of a power system is measured by developing the scenarios of different wind power penetration with different location in the grid [20]. Energy storage system application design is presented for regulating wind power variation and increasing wind energy integration with which the improvement in wind energy integration is between 1,7 % and 8 % [21]. Billinton indicates how to select a wind turbine generator (WTG) which is best suited for a special site to acquire the maximum capacity benefit at the given criterion risk level [22].

After summarizing the advantages and disadvantages of the existing solutions, this paper presents a WFIC optimization model based on the scenario tree construction analysis. This model considers the dynamic process of the power system and applies the scenario tree construction method to deal with the wind speed variable. A hierarchical optimization algorithm that combines w-particle swarm optimization (w-PSO) algorithm and social emotional optimization algorithm (SEOA) is then used to solve the proposed model. The correctness and

validity of this optimization model and the corresponding solution are verified using the IEEE-30 nodes system. The effects of the variation of the correlated factors on the optimization results are also investigated based on the proposed optimization model to offer more valuable information for wind farm programming.

## 2 Wind farm net benefit model

The wind farm integration capacity optimization model is proposed to maximize the economic benefits of wind farms and ensure that the power system is under an economical operating state based on the premise of ensuring the security and stability of the power system by combining the existing control measures and optimization strategies (e.g., minimize grid power loss). This paper presents an optimization model using the wind farm generation net benefit as the objective function, the installation number of WTGs and output power of the dispatched conventional generator units as the decision variables, and the system security operation requirements as model constraints to obtain the solution for optimal integration capacity.

### 2.1 Wind power annual sale benefit

The renewable energy law [23] prioritizes wind power sales and offers a favorable wind power electricity price to encourage renewable development. According to the policy, the total annual electricity sale benefit of wind energy generation is given by

$$B_{SB} = W_{price} \times E_{year} \tag{1}$$

$$E_{year} = \sum_{k=1}^K (p(k) \times \sum_{t=1}^T (H_t \times P_t)) \tag{2}$$

$$P_t = \sum_{f=1}^F \sum_{g=1}^{WGT} N_{fg} \times P_{fg}(\theta_{kt}(j)) \tag{3}$$

$$P_{fg} = \arg \max \{P_{fg}(h), h \in \Phi_{dis}\} \tag{4}$$

where  $B_{SB}$  is the annual electricity sale benefit;  $W_{price}$  is the electricity price for wind power sale;  $E_{year}$  is the annual wind energy generation amount;  $p(k)$  is the probability of the  $k^{th}$  scenario tree;  $H_t$  is the available generation time of the  $t^{th}$  time interval;  $N_{fg}$  is the installation number of the  $g^{th}$  WTG type in the  $f^{th}$  wind farm;  $P_{fg}$  is the optimal output of the  $g^{th}$  WTG type in the  $f^{th}$  wind farm after processing the system optimization dispatch when the wind speed is set to  $\theta_{kt}(j)$ ;  $\theta_{kt}(j)$  is the corresponding wind speed scenario of the  $k^{th}$  scenario tree at the  $t^{th}$  time interval;  $\Phi_{dis}$  is the dispatch solution set corresponding to the  $\theta_{kt}(j)$  scenario; and  $K, T, F$  and  $WGT$  represent the number of scenario tree branches, time intervals, wind farms, and  $WTG$  types, respectively.

### 2.2 Wind farm construction capital cost (WFCCC)

WFCCC is the basic investment cost during the wind farm construction period. The loan mode is usually adopted as the mode of raising money because of the

large amount of initial construction cost. To estimate the annual economic benefit of wind farms, WFCCC must be shared to the whole project period equally so that an equivalent construction capital cost can be considered properly in the benefit calculation. This paper utilizes the capital recovery factor (CRF)[24] to convert WFCCC to the equivalent annual capital cost (EACC). WFCCC using CRF, i.e., EACC, is calculated as follows:

$$C_{EA} = \sum_{f=1}^F \sum_{g=1}^{WGT} \frac{i(1+i)^n}{(1+i)^n - 1} \times C_{Cg} \times N_{fg}, \quad (5)$$

where  $C_{EA}$  is the EACC,  $C_{Cg}$  is the WFCCC of the  $g^{\text{th}}$  WTG type,  $i$  is the loan rate, and  $n$  is the loan term.

### 2.3 Maintenance and operation cost (M&O)

M&O is the cost spent for the promising routine operation of wind farms. It is composed of the equipment repair and maintenance expenses, insurance fees, labor fees, and necessary expenses. M&O is an important part of the wind farm economic benefit calculation considered during an annual time interval. The M&O of wind farms is given by

$$C_{MOA} = \sum_{f=1}^F \sum_{g=1}^{WGT} C_{MOg} \times N_{fg}, \quad (6)$$

where  $C_{MOA}$  is the annual M&O of wind farms, and  $C_{MOg}$  is the annual M&O of the  $g^{\text{th}}$  WTG type.

### 2.4 Wind farm net generation benefit

The wind farm net generation benefit consists of the wind power annual sale benefit, equivalent annual capital cost, and annual maintenance and operation cost. The goal of choosing the wind farm generation benefit as the objective function of the model in this paper is to maximize the economic benefit brought by the wind energy generation. The objective function formula is expressed as follows:

$$\max B_{PB} = \max (B_{SB} - C_{EA} - C_{MOA}). \quad (7)$$

### 2.5 Optimization model constraints

The constraints of the wind farm net benefit model are categorized into equation constraints and inequation constraints. The equation constraints are composed of the active power balance conditions and the reactive power balance conditions, which are expressed as follows:

$$\begin{cases} P_{Gi} + P_{Wi} - P_{Li} - U_i \sum_{j \in i} U_j (G_{ij} \cos \theta_{ij} + B_{ij} \sin \theta_{ij}) = 0 \\ Q_{Gi} + Q_{Wi} - Q_{Li} - U_i \sum_{j \in i} U_j (G_{ij} \sin \theta_{ij} - B_{ij} \cos \theta_{ij}) = 0 \end{cases} \quad (8)$$

where  $P_{Gi}$ ,  $Q_{Gi}$  represent the active output and the

reactive output of the conventional generators at bus  $i$ , respectively;  $P_{Wi}$ ,  $Q_{Wi}$  represent the active output and the reactive output of the wind turbine generators at bus  $i$ , respectively;  $P_{Li}$ ,  $Q_{Li}$  represent the active load and the reactive load at bus  $i$ , respectively;  $U_i$ ,  $U_j$  represent the voltage amplitudes at bus  $i$  and bus  $j$ , respectively;  $\theta_{ij}$  represents the difference in phase angles at bus  $i$  and bus  $j$ ; and  $G_{ij}$ ,  $B_{ij}$  represent conductance and susceptance located in row  $i$  and column  $j$  of system admittance matrix, respectively. The formula formats are assumed above to unify the description of each bus, and they do not indicate that conventional generators, wind turbine generators, and load are connected on each bus simultaneously. The formula format can be changed according to the actual situation.

The inequation constraints are composed of the superior and inferior limit constraints of the decision variables and state variables. The active and reactive power output limits of conventional generators, active power output limits of wind turbine generators, branch power limits, bus voltage limits, and system spinning reserve constraints are considered the variable constraints in this paper, and they are expressed as follows:

$$\begin{cases} P_{Gi}^{\min} \leq P_{Gi} \leq P_{Gi}^{\max}, \\ Q_{Gi}^{\min} \leq Q_{Gi} \leq Q_{Gi}^{\max}, \\ 0 \leq P_{Wi} \leq P_{Wi}^{\max}, \\ 0 \leq S_l \leq S_l^{\max}, \\ U_i^{\min} \leq U_i \leq U_i^{\max}, \\ \sum_{i \in SCG} (P_{Gi}^{\max} - P_{Gi}) \geq P_{res}^{\text{up}}, \\ \sum_{i \in SCG} (P_{Gi} - P_{Gi}^{\min}) \geq P_{res}^{\text{down}}, \end{cases} \quad (9)$$

where  $S_l$  is the branch transmission power;  $SCG$  is the conventional generators set; and  $P_{res}^{\text{up}}$  and  $P_{res}^{\text{down}}$  are the system superior spinning reserve and the system inferior spinning reserve, respectively, which are usually considered as 5 % of the total system load. Superscript max and min represent the superior limits and inferior limits of the corresponding variables, respectively.

## 3 Scenario analysis methodology (SAM)

The main difference between the wind turbine generation mode and the traditional generation mode is the randomness of wind energy. Wind speed variation is difficult to predict and uncontrollable so it brings an obvious uncertainty to the operation and programming of the power system. The probability density function describing the wind speed distribution regularity is a continuous function; thus, it can make the optimization model difficult to be solved if all the possible values are considered, making the model impractical. The scenario analysis methodology [25], a kind of practical

approximate calculation method, discretizes the continuous probability distribution into a series of typical scenarios, with each scenario having a future state possibly appearing. In a special scenario, various influencing factors are ensured. The scenario analysis method can obtain the approximate value of the stochastic variables with different accuracy requirements and is suitable for solving the optimization model, considering the stochastic factors.

### 3.1 Wind speed probability distribution function set

Wind speed is the main factor for deciding wind farm output; thus, describing the variation of wind speed precisely is important. The existing measure is to adopt a single probability distribution function to describe the whole year wind speed. Although this measure can reflect the entire regularity of the annual wind speed variation, it cannot consider the effect caused by short-term and middle-term wind speed variations. The scenario split can only be carried out based on the same probability distribution in the scenario analysis process, which makes the approximation degree of the scenario split degressive and downgrades the optimization results. Therefore, different probability distribution functions corresponding to different variations of wind speed at different time intervals must be adopted for wind speed PDFs to be utilized by the scenario analysis methodology more accurately and to improve the approximation degree of the scenario split and optimization results.

The Weibull distribution can describe the characteristics of wind speed variation appropriately. Using a group of probability distribution parameters instead of a single probability distribution function to describe the variation of annual wind speed can make the description of the probability distribution function more accurate because of the different parameters of the Weibull distribution in different statistical periods (e.g., year, quarter, and month). This paper uses the maximum likelihood principle to solve parameters  $c$  and  $k$ , which are given by the following equations:

$$\sum_{i=1}^n \left[ \frac{1}{k} + \ln V_i - \ln c - \left(\frac{V_i}{c}\right)^k \ln \frac{V_i}{c} \right] = 0, \tag{10}$$

$$\sum_{i=1}^n \left[ -\frac{k}{c} + \frac{k}{c} \left(\frac{V_i}{c}\right)^k \right] = 0, \tag{11}$$

where  $V_i$  is the sampling values of wind speed in the statistical period,  $c$  and  $k$  are the scale parameter and the shape meter of the Weibull distribution, respectively. The iteration method is used to solve Eq. (10) and Eq. (11).

### 3.2 "Wind Speed–Power" scenario split

According to section 3.1, the format of the probability distribution function set describing the annual wind speed variation regularity is  $\{(c_1, k_1), (c_2, k_2), \dots, (c_i, k_i), \dots\}$ , where  $(c_i, k_i)$  presents one possible value of the Weibull distribution parameters. After the parameter sets are acquired, the scenario split of the annual wind speed and

the corresponding wind power value calculation can be processed using the scenario analysis methodology.

Fig. 1 shows the sketch map of the wind speed probability distribution function discretization. The wind speed coordinate interval of the probability distribution function is discretized into  $N$  segment smaller intervals with a given discretization interval and a given start coordinate on the horizontal axis of the probability distribution function. The reasonableness of the discretization method has an important role in appropriately reflecting the regularity of the wind speed variation. Therefore, a suitable discretization interval and coordinate locations must be chosen to make the discretization values set the approximate original probability distribution function satisfactorily. This paper adopts the following discretization principles summarized from engineering experience: by choosing cut-in speed  $v_{ci}$ , rated speed  $v_R$ , and cut-out speed  $v_{co}$  of the wind turbine generator as the three characteristic coordinate values on the horizontal axis for discretization, the whole wind speed interval is split into four segments first. Focusing on interval  $[v_{ci}, v_R]$ , by choosing the standard deviation  $\sigma_t$  of the wind speed PDF discretized as the discretization interval and by using formula  $n = \frac{v_R - v_{ci}}{\sigma_t}$  plus Tab. 1

to ensure the number of discrete segments, the interval  $[v_{ci}, v_R]$  is discretized further. After completing the two steps, the final scheme of the wind speed interval discretization is acquired.

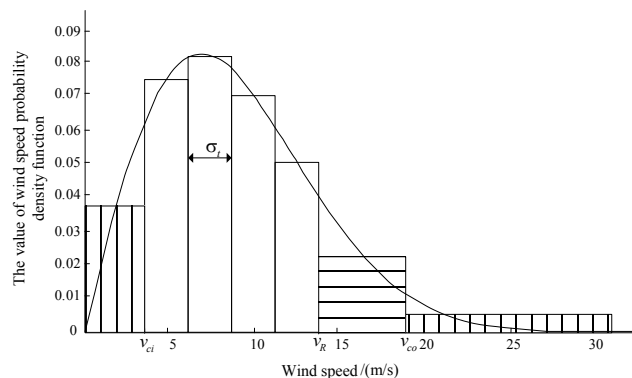


Figure 1 Discretization of the wind speed probability distribution function

Table 1 Principle of determining the discretization number

| $n$           | Number of Discrete Segments           |
|---------------|---------------------------------------|
| $\geq 2$      | Rounding ( <b>splitting equally</b> ) |
| $<2$ and $>1$ | <b>2 (split equally)</b>              |
| $\leq 1$      | 1                                     |

This discretization method is called the asymmetrical interval discretization method, in which wide interval discretization is adopted in large and small wind speed regions, and  $\sigma_t$ -interval and equation discretization is adopted in the middle wind speed region to highlight the main scenarios and reduce the calculation work associated with infrequent scenarios. The approximation acquired by the scenario split method is desirable through which the optimal mathematical expectation value of the objective function can be obtained satisfactorily.

The discrete random variable  $\theta_{kt}(j)$  denotes the discrete wind speed scenarios acquired by SAM, where  $j$

$= 1, \dots, J$  denotes the number of split intervals.  $E(P_{jkt})$  is the mathematical expectation value of the scenario power corresponding to interval  $j$ . The deduction of the expectation value calculation formula is described in detail in section 3.3, in which the output value of the single WTG corresponding to the interval  $j$  is calculated. The probability  $p(j_{kt})$  of choosing scenario  $\theta_{kt}(j)$  is equal to the definite integration of wind speed PDF over interval  $j$ . The formula is expressed as follows:

$$p(j_{kt}) = \frac{\overline{\theta_{kt}(j)}}{\underline{\theta_{kt}(j)}} \int f(V) dV, \tag{12}$$

where  $\underline{\theta_{kt}(j)}$  and  $\overline{\theta_{kt}(j)}$  represent the wind speed values corresponding to the left and right ends of the interval  $j$ , respectively.

After dealing with the wind speed scenario set by Eq. (12), the continuous monthly probability distribution set of the wind speed is converted to a discrete monthly scenario power set. An annual scenario power branch is described with a monthly scenario power series, which is composed of different monthly scenario powers chosen from the corresponding monthly scenario power sets. Suppose that there are  $K$  annual scenario power branches denoted as  $S_k$  ( $k = 1, \dots, K$ ), the number of scenarios in the monthly scenario power set is  $J_t$ , and the scenario power value is denoted as  $E(P_{jkt})$ , the set format expression of  $S_k$  is given by

$$S_k = \{E(P_{jkt_1}), \dots, E(P_{jkt_2}), \dots, E(P_{jkt_{J_t}})\}, \tag{13}$$

where  $t$  is the time circle (i.e., the month in this paper), and  $S_k$  is the annual scenario power branch. The set composed of all  $S_k$  is called the scenario tree:  $Tree = \{S_1, S_2, \dots, S_K\}$ . The process of constructing the scenario tree is shown in Fig. 2. After completing the scenario tree construction, the probability  $p(k)$  of each  $S_k$  must be calculated using Eq. (14):

$$p(k) = \prod_{t=1}^T p(j_{kt}). \tag{14}$$

The calculation process is repeated until all branch probabilities in the scenario tree are obtained. In this study, the whole "wind speed–power" scenario split is accomplished.

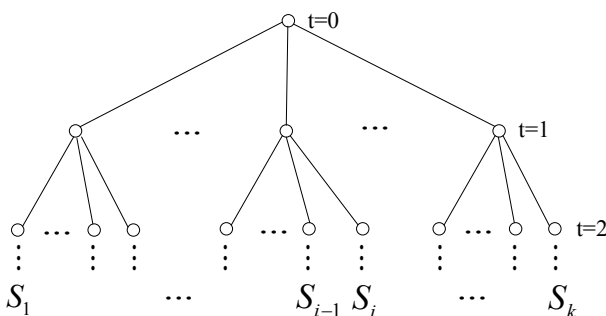


Figure 2 Scenario tree construction process

### 3.3 Formula deduction of the WTG – scenario power calculation

After acquiring the wind speed interval discretization scheme, the corresponding scenario power values in each split subinterval are calculated. The main point of this section is to determine the function relation between the left and right ends of the wind speed values  $v_{left}$ ,  $v_{right}$  of the split subinterval, wind speed PDF  $f(V)$ , and the corresponding subinterval scenario power  $E(P_{jkt})$ . Eq. (15) shows the function relation between the single WTG output and wind speed:

$$P_W = \begin{cases} 0 & (V < v_{ci} \cup V > v_{co}) \\ \frac{V^3 - v_{ci}^3}{v_R^3 - v_{ci}^3} & (v_{ci} \leq V \leq v_R) \\ P_R & (v_R < V < v_{co}) \end{cases}, \tag{15}$$

where  $v_{ci}$ ,  $v_R$ ,  $v_{co}$  and  $P_R$  represent the cut-in wind speed, rated wind speed, cut-out wind speed, and rated power, respectively.

Suppose  $[v_{left}, v_{right}] \subset [v_{ci}, v_R]$ , we have  $P_{left} = P_W(v_{left})$ ,  $P_{right} = P_W(v_{right})$  based on Eq. (15). According to probability theory, the expectation value of the WTG output corresponding to this subinterval is

$$E(P_{jkt}) = \frac{\int_{P_{left}}^{P_{right}} P_W f_{P_W}(P_W) dP_W}{\int_{P_{left}}^{P_{right}} f_{P_W}(P_W) dP_W}. \tag{16}$$

The PDF of the WTG output  $f_{P_W}(P_W)$  in Eq. (16) is unknown, so the expectation value of the scenario power cannot be calculated directly. The solution is to replace the unknown PDF with the known PDF, enabling the transformed formula format to be calculated.

Eq. (15) is a monotonic increasing function, indicating that each WTG output value must correspond to a unique wind speed. According to this conclusion, the mathematical relation between WTG output and wind speed is a single mapping, i.e., the stochastic variation process of the WTG output is in accordance with that of the corresponding wind speed. Therefore, the stochastic process of  $P_W$  at interval  $[P_{left}, P_{right}]$  is equal to that of  $V$  on the interval  $[v_{left}, v_{right}]$ . With the premise of knowing the wind speed PDF  $f(V)$ , if  $P_W$  is considered as the function of variable  $V$ , the solution for the WTG output expectation value  $E(P_{jkt})$  can be converted to the solution for the expectation value of  $P_W(V)$ , which is the function of stochastic variable  $V$ . Therefore,  $E(P_{jkt})$  can be solved using the wind speed PDF  $f(V)$  in the value space of variable  $V$ .

According to the equal relations analyzed above, the deduction of the expectation value formula is given as follows. Define coefficients  $k_1$ ,  $k_2$  with the corresponding expressions:

$$k_1 = \frac{P_R}{v_R^3 - v_{ci}^3}, k_2 = -\frac{v_{ci}^3}{v_R^3 - v_{ci}^3} P_R, \text{ respectively.}$$

Substitute the coefficient expressions and Eq. (15) into Eq. (16):

$$E(P_{jkt}) = k_1 \frac{\int_{v_{\text{right}}}^{v_{\text{left}}} v^3 f(V) dV}{\int_{v_{\text{right}}}^{v_{\text{left}}} f(V) dV} + k_2. \tag{17}$$

Eq. (17) is the WTG scenario power calculation formula.

#### 4 Solution algorithm of the optimization model

##### 4.1 SEOA

SEOA[26] simulates the whole procedure in which, under the rational emotion state, an individual perceives the evaluations coming from the surrounding circumstance and adopts the corresponding actions to direct the next step operation according to the emotional feedback mode to search for the optimal objective using advanced intelligent simulation (AIS). Introducing AIS into SEOA, local information can be utilized more adequately to find better results. SEOA has been verified to possess good optimization performance in standard function testing.

In SEOA, each individual represents a virtual person. The mapping that considers emotion as input and action as output is obtained using individual emotion variation as the control strategy. The action mode is chosen according to the corresponding emotion index in each iteration process, and the emotional evaluation value is used to evaluate the operation effect of the chosen action mode. The emotion index can increase with the positive operation effect, or it can decrease. Suppose  $E_j(t)$  is the emotion index of individual  $j$  in a virtual population, and  $\bar{x}_j(t)$  is the corresponding social evaluation. The original emotion indexes of each individual are set to 1, which defaults the original states that each individual is optimum. SEOA is updated through the following steps. At the beginning of the algorithm operation, the individual social evaluations are denoted as  $\bar{x}_j(0)$ , and the first iteration formula is given by

$$\bar{x}_j(1) = \bar{x}_j(0) - c_3 \times rand_3 \times \sum_{s=1}^L (\bar{x}_s(0) - \bar{x}_j(0)), \tag{18}$$

where  $c_3$  is the weight coefficient reflecting the effect of weak individuals,  $rand_3$  is a random number following the uniform distribution, and  $L$  are the last  $L$  individuals having the  $L$  lowest social evaluations.

In the  $t^{\text{th}}$  iteration, a new emotion index of each individual is calculated with the emotion index formula, followed by the known social evaluation value of each individual. Subsequently, the new emotion index is compared with the emotion index threshold value to choose the appropriate action update formula for updating the social evaluation of each individual, calculate the corresponding social evaluation values, and update the best evaluation of each individual as well as that of the whole population. Iteration includes the whole process described above, and it will not be stopped until the termination conditions are satisfied. The detailed action

update formulae are as follows.

This paper adopts the emotion index formulae based on the first emotional intensity law shown by Eq. (19):

$$\begin{cases} E_j(t+1) = k \cdot \lg(1 + \Delta f_j), \\ \Delta f_j = \frac{|f_j - \bar{f}|}{\max(|f_{\text{best}} - \bar{f}|, |f_{\text{worst}} - \bar{f}|)}, \end{cases} \tag{19}$$

where  $k$  represents the intensity coefficient;  $\Delta f_j, f_j, \bar{f}, f_{\text{best}}$  and  $f_{\text{worst}}$  represent the social evaluation value difference of individual  $j$  in the  $t^{\text{th}}$  iteration, social evaluation value of individual  $j$ , average social evaluation value of the whole population, best individual social evaluation value in the population, and the worst individual social evaluation value in the population in the  $t^{\text{th}}$  iteration, respectively.

According to the number relation between the individual emotion index and the emotion index threshold value, the action update mode is chosen using the following rules:

(1) When  $E_j(t+1) < m_1$ , an individual mainly focuses on the population optimal information study:

$$\bar{x}_j(t+1) = \bar{x}_j(t) + c_2 \times rand_2 \times (\overrightarrow{App}_{\text{best}}(t) - \bar{x}_j(t)), \tag{20}$$

where  $\overrightarrow{App}_{\text{best}}(t)$  represents the best historical social evaluation of the population as follows:

$$\overrightarrow{App}_{\text{best}}(t) = \arg \min_s \{f(\bar{x}_s(h)) | 1 \leq h \geq t\}. \tag{21}$$

(2) When  $m_1 < E_j(t+1) < m_2$ , an individual conducts a self-study and a population optimal evaluation study simultaneously:

$$\begin{aligned} \bar{x}_j(t+1) = & \bar{x}_j(t) + c_1 \times rand_1 \times (\bar{x}_{j_{\text{best}}}(t) - \bar{x}_j(t)) + \\ & + c_2 \times rand_2 \times (\overrightarrow{App}_{\text{best}}(t) - \bar{x}_j(t)) - \\ & - c_3 \times rand_3 \times \sum_{s=1}^L (\bar{x}_s(t) - \bar{x}_j(t)), \end{aligned} \tag{22}$$

where  $\bar{x}_{j_{\text{best}}}(t)$  represents the best historical social evaluation of an individual  $j$  as follows:

$$\bar{x}_{j_{\text{best}}}(t) = \arg \min \{f(\bar{x}_j(h)) | 1 \leq h \geq t\}. \tag{23}$$

(3) When  $E_j(t+1) > m_2$ , an individual mainly focuses on the study of self information:

$$\begin{aligned} \bar{x}_j(t+1) = & \bar{x}_j(t) + c_1 \times rand_1 \times (\bar{x}_{j_{\text{best}}}(t) - \bar{x}_j(t)) + \\ & - c_3 \times rand_3 \times \sum_{s=1}^L (\bar{x}_s(t) - \bar{x}_j(t)), \end{aligned} \tag{24}$$

where  $m_1, m_2$  are the superior and inferior limits of the

emotion index threshold value, respectively. The meaning of the other symbols has been explained previously.

**4.2 Solution flow of the optimization model**

This paper adopts the hierarchical optimization algorithm, which combines the w-PSO algorithm and SEOA, to solve the optimization model. The inner layer optimization mainly focuses on the solution of wind farm optimal output with system dispatch. The inner layer optimization results significantly affect the ultimate optimization results and the inner layer optimization process involving power flow calculation. The constraints judgment is also complicated. Therefore, SEOA, which possesses better optimization performance, is adopted to solve the inner layer optimization model. The outer layer optimization focuses on the wind farm benefit and the correlative economic parameters optimization based on the inner layer optimization results. The process of outer layer optimization is easier when no power flow calculation and constraints judgment exist. The w-PSO algorithm is adopted for the outer layer optimization to improve the whole optimization efficiency without affecting the ultimate optimization results.

According to the idea of hierarchy optimization described above, the solution flow of the WFIC optimization model based on the scenario tree construction method is as follows:

1) Eq. (10) and Eq. (11) are utilized to calculate parameter  $c$ ,  $k$  of the monthly wind speed PDF. The annual wind speed PDF parameter set is deduced as  $\{(c_1, k_1), (c_2, k_2), \dots, (c_i, k_i), \dots\}$ .

2) The annual scenario power tree is calculated  $Tree = \{S_1, S_2, \dots, S_K\}$  as well as the corresponding probability  $p(k)$  using the scenario analysis method.

3) Generating the initial population

The conventional generator output, bus voltage of the conventional generator, number of installed WTGs, and type of WTGs are chosen as the control variables to constitute the searching space of a virtual person  $[P_G, V_G, N_W, T_W]$ . In the searching space,  $N_W$  and  $T_W$  are the control variables of the outer layer optimization, and the rest are the control variables of the inner layer optimization. The control variables  $N_W, T_W$  of the outer layer optimization with a given number of the population are generated from the variable value spaces to be the initial population of the outer layer optimization model. The initial outer layer population is converted into the initial conditions of the inner layer optimization model with the scenario analysis results, and the initial control variables  $P_G, V_G$  of the inner layer optimization are generated to obtain the initial population of the inner layer optimization model. The two initial populations are integrated to obtain the complete initial social evaluation of the optimal wind power integration capacity model.

4) Initial iteration of the solution algorithm

Eq. (18) is used to update the social evaluation  $x_j$  of individual  $j$  and calculate the social evaluation value  $f_j$ .

5) The emotion index threshold  $m_1, m_2$  is set, and the emotion index  $E_j(t)$  of each individual is calculated using Eq. (19) according to the social evaluation value  $f_j$  of the last iteration.

6) Eq. (20) to Eq. (24) are used to update the social evaluation  $x_j$  of individual  $j$  and calculate the social evaluation value  $f_j$  according to the new emotion index  $E_j(t)$ .

7) The best historical social evaluation  $\bar{x}_{jbest}(t)$  of individual  $j$  and the best historical social evaluation  $\overrightarrow{App}_{best}(t)$  of the whole population are updated.

8) The termination conditions are verified whether they satisfy the inner layer optimization. If it is satisfied, the optimal output is given and the inner layer optimization is finished; otherwise, the program goes back to step 5 to continue searching.

9) After finishing the inner layer optimization, the outer layer optimization begins the searching process by updating the rules of the w-PSO algorithm on the premise of the inner layer optimization results.

10) The global optimization results are verified whether they satisfy the termination conditions of WFIC optimization model. If they are satisfied, the terminate optimization output is given and the whole optimization model is solved; otherwise, the program goes back to step3 to continue searching until all the conditions are satisfied.

**5 Case studies**

Case studies on the IEEE-30 nodes system are presented to verify the correctness and availability of the proposed optimization model and the solution algorithm in this paper. The effects of the correlative factors affecting the determination of WFIC are also investigated. The test system includes 6 conventional generators and 41 transmission lines. The power grid topology, transmission line parameters, and conventional generator parameters are from the standard system data. The system loads adopt the dynamic load per-unit values of 12 months. The parameters of the wind turbine generator for the study are shown in Tab. 2 [19, 27]. The parameters shown in Tab. 2 are the data of typical WTG types, which are used to illustrate the feasibility and universality of proposed optimization model in the article.

**Table 2** Wind turbine generator type and parameter

| Type | $P_R$<br>MW | $v_{ci}$<br>m/s | $v_R$<br>m/s | $v_{co}$<br>m/s | $C_C$<br>kUSD/MW | $C_{MO}$<br>kUSD/MW/a |
|------|-------------|-----------------|--------------|-----------------|------------------|-----------------------|
| A    | 0,5         | 2,7             | 12,4         | 19,3            | 1220             | 29                    |
| B    | 2           | 3,4             | 8,4          | 15,3            | 1100             | 32                    |
| C    | 1           | 3,9             | 11,1         | 25              | 1150             | 33                    |
| D    | 0,1         | 4,3             | 7,7          | 17,9            | 1250             | 30                    |

Statistical data are the measured wind speed data from the Yumen wind farm in Gansu. The wind speed PDF parameters and characteristic indexes are calculated with a monthly time interval based on the statistical data. The parameter and characteristic index calculation results of each month are shown in Tab. 3.

Tab. 3 shows that an obvious difference exists between the wind speed PDF parameters and the characteristic indexes of each month. Therefore, using a single wind speed PDF to describe the annual wind speed probability distribution is not accurate. Calculating the monthly wind speed PDF parameters to obtain the annual

parameter set can make the monthly wind speed PDF parameters more appropriate and reduce the effect to ultimate optimization results caused by the description error of distribution regularity.

**Table 3** Monthly wind speed PDF parameters and characteristic indexes

| Month | <i>c</i> / m/s | <i>k</i> | <i>v</i> / m/s |
|-------|----------------|----------|----------------|
| 1     | 6,96           | 1,83     | 3,51           |
| 2     | 7,32           | 1,55     | 4,33           |
| 3     | 9,66           | 2,16     | 4,17           |
| 4     | 10,39          | 2,40     | 4,09           |
| 5     | 7,89           | 2,09     | 3,51           |
| 6     | 7,68           | 2,03     | 3,51           |
| 7     | 8,48           | 2,12     | 3,73           |
| 8     | 7,11           | 1,81     | 3,60           |
| 9     | 8,04           | 1,86     | 3,99           |
| 10    | 6,83           | 1,92     | 3,29           |
| 11    | 7,16           | 1,81     | 3,64           |
| 12    | 7,82           | 1,79     | 4,01           |

This paper chooses the wind farm net generation benefit as an objective function to solve the proposed optimization model and determine the optimal WTG integration capacity scheme. Moreover, the effects caused by the variation of wind farm integration location, the number of wind farm integration, WTG style, and reactive output limit of conventional generator are studied:

(A) Single bus 4, 14, 19, 24, 28, and 29 as well as bus set 14–29, 24–29, and 28–29 are chosen as the wind farm integration bus. The annual wind speed PDF parameter set is shown in Tab. 3. The power limit of the transmission line is 50 MV·A, the bus voltage range is 0,95 p.u. to 1,05 p.u., the WTG style is a double-fed induction generator (DFIG) with a constant power factor control strategy, and the power factor is set to 0,95. The optimal integration powers of the WTG of different types on different single buses are shown in Tab. 4. The optimal WTG integration capacity construction schemes and correlative economic indexes of each single bus are

presented in Tab. 5. Tab. 6 shows the optimal WTG type combinations and corresponding integration powers of different bus sets under the multiple-bus integration mode. Tab. 7 shows the optimal WTG integration capacity construction schemes and the correlative economic indexes of different bus sets.

Tab. 4 shows that optimal integration powers are considerably different with different integration buses for the same WTG type, and the optimal integration powers of different WTG types are also considerably different in the same integration bus. The reason for the first phenomenon is that WTGs integrated from different buses change the system grid configuration and power flow distribution, and the equivalent WTG model integrated from the same bus for the second phenomenon is changed because of the difference in parameters of the different WTG types. The previous analysis illustrates that the variation of the integration bus and WTG type can have an obvious effect on the ultimate optimization results. Therefore, the optimal integration capacities of each WTG type on each candidate bus should be calculated to determine the ultimate optimal integration bus and WTG type scheme in the wind farm planning stage.

The optimal WTG types determined by the wind energy generation net benefit in Tab. 5 and the average integration power in Tab. 4 are both type D WTG. The reason for choosing type D is that the wind speed difference of type D WTG between rated wind speed and cut-in wind speed is minimal according to the WTG parameters. Therefore, the effect of disturbance caused by wind speed variation is minimal; i.e., the utilization efficiency and the average integration power of type D WTG are maximal under the same wind speed circumstance. Furthermore, there are only a few differences between the investment costs and the M&O costs of each WTG type so the generation net benefit of type D WTG is also at maximum.

**Table 4** Optimal average integration power in case A

| Integration bus | Optimal average integration power of different types of WTG/MW |        |        |        |
|-----------------|--|--------|--------|--------|
|                 | A  | B      | C      | D      |
| 4               | 24,906   | 44,322 | 30,062 | 45,972 |
| 14              | 19,804   | 35,247 | 23,897 | 36,847 |
| 19              | 25,244   | 44,802 | 30,506 | 46,803 |
| 24              | 27,853   | 48,514 | 33,539 | 51,040 |
| 28              | 23,375   | 41,130 | 28,141 | 43,192 |
| 29              | 10,148   | 18,535 | 12,681 | 19,229 |

**Table 5** WTG construction scheme and economic indexes in case A

| Bus                                  | 4     | 14    | 19    | 24    | 28    | 29    |
|--------------------------------------|-------|-------|-------|-------|-------|-------|
| WTG type                             | D     | D     | D     | D     | D     | D     |
| Installation number                  | 907   | 725   | 918   | 1 017 | 850   | 390   |
| Installation capacity / MW           | 90,7  | 72,5  | 91,8  | 101,7 | 85    | 39    |
| Capital cost / 10 <sup>8</sup> USD   | 1,134 | 0,906 | 1,148 | 1,271 | 1,063 | 0,488 |
| M&O cost / 10 <sup>6</sup> USD/a     | 2,721 | 2,175 | 2,754 | 3,051 | 2,55  | 1,17  |
| Sale benefit / 10 <sup>7</sup> USD/a | 3,552 | 2,847 | 3,616 | 3,944 | 3,337 | 1,486 |
| Net benefit / 10 <sup>7</sup> USD/a  | 1,948 | 1,565 | 1,992 | 2,145 | 1,834 | 0,796 |

The influencing factors affecting the generation net benefit include not only the integration power of WTG, but also the available generation time, electricity price for wind power sale, investment cost, M&O cost, and so on. Thus, the optimal WTG type determined by the

generation net benefit is not always the same as the type determined by the average integration power for any integration bus. When there is no large difference in other influencing factors, except for the integration power of WTG, the optimal WTG types determined from the two



different angles are possibly the same. The variation tendency of these two variables is the same, i.e., the generation net benefit increases when the average integration power increases.

Tab. 6 shows that the sum of the average integration powers of the different integration bus sets is different; the average integration powers of each bus in the same integration bus set are also obviously different. However, for the same integration bus, the change in the integration bus set the concerned bus belongs to has little effect on the optimal integration power of the concerned bus, such as bus 29 in Tab. 6. The reason is that the influencing factors of the integration powers of the candidate buses are the system grid topology and the operation conditions. The integration powers of the candidate buses will not fluctuate drastically as long as there are no obvious changes on the grid topology and operation conditions.

The integration powers of bus 24 and bus 29 in the multiple-bus integration mode are less than those of bus 24 and bus 29 in the single-bus integration mode. This difference illustrates that different bus integration modes can change the grid topology, resulting in the change in the integration powers of the candidate buses. Although there are some losses on the integration power of the candidate bus itself in the multiple-bus integration mode, the total integration power of the bus set is greater than the optimal integration power of any bus in the bus set in a single-bus integration mode. This finding proves that the multiple-bus integration mode can improve the total integration power of wind farms and that there is no obvious effect caused by the local loss on the ultimate optimization results. The data in Tab. 7 illustrate that the generation net benefit increases by at least 4,36 million USD in the multiple-bus mode.

**Table 6** Optimal average integration power in the multiple-bus integration mode in case A

| Integration bus set | Bus number | WTG type | Optimal average integration power / MW | Total average integration power / MW |
|---------------------|------------|----------|--|--------------------------------------|
| Bus24+29            | 24         | D        | 47,036                                 | 62,193                               |
|                     | 29         | B        | 15,157                                 |                                      |
| Bus14+29            | 14         | B        | 30,803                                 | 48,112                               |
|                     | 29         | D        | 17,308                                 |                                      |
| Bus28+29            | 28         | D        | 33,094                                 | 48,160                               |
|                     | 29         | B        | 15,066                                 |                                      |

**Table 7** WTG construction scheme and economic indexes in the multiple-bus integration mode in case A

| Integration bus set                   | Bus 24+29 |        | Bus 14+29 |        | Bus 28+29 |        |
|---------------------------------------|-----------|--------|-----------|--------|-----------|--------|
|                                       | Bus 24    | Bus 29 | Bus 14    | Bus 29 | Bus 28    | Bus 29 |
| WTG type                              | D         | B      | B         | D      | D         | B      |
| Installation number                   | 950       | 17     | 34        | 361    | 656       | 17     |
| Installation capacity / MW            | 129       |        | 104,1     |        | 99,6      |        |
| Capital cost / $10^8$ USD             | 1,5581    |        | 1,1925    |        | 1,1906    |        |
| M&O cost / $10^6$ USD/a               | 3,938     |        | 3,259     |        | 3,056     |        |
| Sale benefit / $10^7$ USD/a           | 4,8053    |        | 3,7173    |        | 3,721     |        |
| Generation net benefit / $10^7$ USD/a | 2,5806    |        | 1,9902    |        | 2,0165    |        |

(B) The generator style of WTG is changed into the common asynchronous induction generator, which is widely used in wind energy generation systems. Bus 4, 28, and 29 are chosen as the integration buses to solve the optimization model; the optimization results are compared with those of the same buses in case A. The effect of the variation of the system reactive power supply on the ultimate optimization results is illustrated by the simulation of reducing the reactive output superior limit of the conventional generators by 25 Mvar in the test system. The remaining calculation conditions are the same as those in case A. The optimal integration powers with asynchronous generator condition are shown in Tab. 8. The WTG integration capacity construction scheme and the correlative economic indexes are presented in Tab. 9.

Comparing Tab. 4 with Tab. 8, the change in generator style has a different effect on the variation of the optimal integration powers of different integration buses. The integration powers of the WTG of different types on bus 4 remain approximately the same. The integration powers of the WTG of different types on bus 28 are reduced. The integration powers of WTG of different types on bus 29 increase drastically. The reason for this phenomenon is that asynchronous generator integration reduces the reactive power resource and

increases the reactive power load simultaneously. Furthermore, different WTG integration buses correspond to different system topologies. The connection of different integration buses with the asynchronous generator style generates different results. When the integration bus is appropriate, the distribution of the reactive power supply and demand is balanced so there is no obvious fluctuation on the integration power. When the integration bus is located in a heavy reactive power load area or reactive power resource area, the whole load distribution and the power flow distribution change, resulting in the increase or decrease in the integration power of the candidate buses.

The economic benefit variation tendency in Tab. 5 and Tab. 9 is the same as that of the integration power variation: there is no obvious difference in the benefit of bus 4; the benefit of bus 28 decreases slightly; the benefit of bus 29 increases drastically. Although the integration power of bus 4 increases slightly under the asynchronous generator style integration, the installation number of the determined type D WTG increases to 944 from 907, resulting in the increase in the corresponding capital cost and M&O cost. The ultimate optimization result shows that the generation net benefit of the asynchronous generator mode is less than that of the DFIG mode, the

difference of which is USD 426 000. This result illustrates that the generation net benefit does not increase as soon as the integration power increases but that the total

investment cost of WTG should be considered to determine the final generation net benefit.

**Table 8** Optimal average integration power(original Q limits)

| Integration bus | Optimal average integration power of different types of WTG/MW |        |        |        |
|-----------------|--|--------|--------|--------|
|                 | A  | B      | C      | D      |
| 4               | 25,106   | 44,454 | 30,542 | 46,272 |
| 28              | 21,264   | 36,984 | 25,357 | 38,485 |
| 29              | 15,389   | 26,970 | 18,339 | 27,601 |

**Table 9** WTG construction scheme and economic indexes (original Q limits)

| Bus                                  | Bus 4  | Bus 28 | Bus 29 |
|--------------------------------------|--------|--------|--------|
| WTG type                             | D      | D      | B      |
| Installation number                  | 944    | 786    | 30     |
| Installation capacity / MW           | 94,4   | 78,6   | 60     |
| Capital cost / 10 <sup>8</sup> USD   | 1,18   | 0,9825 | 0,654  |
| M&O cost / 10 <sup>6</sup> USD/a     | 2,832  | 2,358  | 1,92   |
| Sale benefit / 10 <sup>7</sup> USD/a | 3,5751 | 2,9735 | 2,0838 |
| Net benefit / 10 <sup>7</sup> USD/a  | 1,9054 | 1,5833 | 1,1234 |

The optimal integration powers, WTG integration capacity construction schemes, and correlative economic indexes are shown in Tab. 10 and Tab. 11, respectively, after changing the reactive output superior limit conditions. The comparison of the calculation results before and after the reactive power superior limits change shows that when the reactive power superior limits decrease, the optimal integration powers of each WTG type on each candidate bus in the asynchronous generator

mode decrease, and the corresponding generation net benefits also decrease. Therefore, the effect caused by the system reactive power supply margin and the reactive power resource location should be considered in the wind farm planning stage, and the integration power losses, added costs of improving the reactive power supply ability, and generation net benefit losses should be considered comprehensively to ensure that the system integrated benefit is maximized.

**Table 10** Optimal average integration power(Q limits reduction)

| Integration bus | Optimal average integration power of different types of WTG/MW |        |        |        |
|-----------------|--|--------|--------|--------|
|                 | A  | B      | C      | D      |
| 4               | 20,476   | 38,089 | 25,716 | 39,631 |
| 28              | 16,143   | 30,128 | 19,986 | 30,323 |
| 29              | 10,618   | 19,316 | 13,168 | 19,992 |

**Table 11** WTG construction scheme and economic indexes (Q limits reduction)

| Bus                                  | Bus 4  | Bus 28 | Bus 29 |
|--------------------------------------|--------|--------|--------|
| WTG type                             | B      | D      | B      |
| Installation number                  | 46     | 675    | 24     |
| Installation capacity / MW)          | 92     | 67,5   | 48     |
| Capital cost / 10 <sup>8</sup> USD   | 1,0028 | 0,8438 | 0,5232 |
| M&O cost / 10 <sup>6</sup> USD/a     | 2,944  | 2,025  | 1,536  |
| Sale benefit / 10 <sup>7</sup> USD/a | 2,9429 | 2,3428 | 1,4925 |
| Net benefit / 10 <sup>7</sup> USD/a  | 1,4702 | 1,1489 | 0,7241 |

The changes in wind turbine generator style and conventional generator reactive output limit also make the WTG type determined by the optimal integration power different from the type determined by the optimal generation net benefit. For example, the WTG type determined by the optimal integration power on bus 29 is type D in Tab. 8, whereas the WTG type determined by the optimal generation net benefit on bus 29 is type B in Tab. 9, these two types are not the same.

(C) The effects on the optimization results brought by the variation of WTG economic parameters are studied under the condition that the investment cost of type B WTG increases by 1 percent of the original cost, and the grid topologies and operation conditions are the same as those of the multiple-bus integration mode in case A. The optimal integration powers, WTG integration capacity construction schemes, and correlative economic indexes

are shown in Tab. 12 and Tab. 13, respectively, after increasing the investment cost.

Comparing the calculation results before and after changing the investment cost together, the determined WTG types of the three candidate bus sets before and after cost change are all type D or type B, and they have superior integration power performance in the single-bus integration mode. This result illustrates that, although the WTG types determined by the optimal generation net benefit are not always the same as those determined by the optimal integration power, the types must be those possessing superior integration power performance. According to the comparison of economic indexes and determined WTG types, the optimization results are prone to the WTG types with lower relative economic costs. The relative cost of type B WTG is lower before its investment cost increases so type B WTG is more likely

to be chosen. Furthermore, the generation net benefits of each bus set before the investment cost increases are superior. The relative cost of type B WTG increases after its investment cost increases, making type D WTG more advantageous. The increase in investment cost makes the

generation net benefit of each bus set decrease compared with that before the cost increases. Therefore, improving the utilization efficiency and decreasing the investment cost of WTG can help improve the final generation net benefit.

**Table 12** Optimal average integration power in the multiple-bus integration mode (investment cost increase)

| Integration bus set | Bus number | WTG type | Optimal average integration power / MW | Total average integration power / MW |
|---------------------|------------|----------|--|--------------------------------------|
| Bus 24+29           | 24         | D        | 47,036                                 | 62,136                               |
|                     | 29         | D        | 15,1                                   |                                      |
| Bus 14+29           | 14         | D        | 31,189                                 | 48,497                               |
|                     | 29         | D        | 17,308                                 |                                      |
| Bus 28+29           | 28         | D        | 33,094                                 | 48,160                               |
|                     | 29         | B        | 15,066                                 |                                      |

**Table 13** WTG construction scheme and economic indexes in the multiple-bus integration mode (investment cost increase)

| Integration bus set                   | Bus 24+29 |        | Bus 14+29 |        | Bus 28+29 |        |
|---------------------------------------|-----------|--------|-----------|--------|-----------|--------|
|                                       | Bus 24    | Bus 29 | Bus 14    | Bus 29 | Bus 28    | Bus 29 |
| WTG type                              | D         | D      | D         | D      | D         | B      |
| Installation number                   | 950       | 307    | 636       | 361    | 656       | 17     |
| Installation capacity / MW            | 125,7     |        | 99,7      |        | 99,6      |        |
| Capital cost / $10^8$ USD             | 1,5713    |        | 1,2463    |        | 1,194     |        |
| M&O cost / $10^6$ USD/a               | 3,771     |        | 2,991     |        | 3,056     |        |
| Sale benefit / $10^7$ USD/a           | 4,8009    |        | 3,7471    |        | 3,721     |        |
| Generation net benefit / $10^7$ USD/a | 2,5774    |        | 1,9836    |        | 2,0125    |        |

## 6 Conclusion

This paper presents an optimization model for determining the wind farm optimal integration capacity by taking the maximization of wind farm generation net benefit as the objective function. A hierarchical optimization algorithm, which combines the w-PSO algorithm and SEOA, is then adopted to solve the proposed optimization model. This optimization model considers the effects caused by the annual load dynamic process, security operation constraints, output power constraints of the generator units, wind power sale price, and wind farm investment cost comprehensively. Furthermore, the model also considers the randomness of wind farm power output. The scenario analysis method is used to deal with the random wind power using the PDF parameter set to describe the annual wind speed probability distribution, establishing the discretization principles of wind speed probability distribution and providing the scenario tree construction method of wind power output in this model.

Case studies adopt IEEE-30 nodes system as the test system to verify the correctness of the optimization model and the validity of solving algorithms, and discuss the effects caused by the variation of wind farm integration location and number, WTG style, reactive output limit of conventional generator units, and WTG investment cost. The calculation results illustrate that there are obvious differences among the wind farm optimal integration capacities integrated from different integration buses; corresponding generation net benefits are also different. The multiple-bus integration mode can improve the total integration capacity and increase the economic benefit of wind farms. The variation of the generator style and the reactive output limit of the generator unit also affect the integration capacity of the wind farm. The asynchronous generator integration and the reduction of reactive output

limit are equal to the increase in the system reactive power demand. Therefore, the system reactive power supply margin and the reactive power resource location should be considered in the wind farm planning stage to avoid limiting the integration capacity of the wind farm because of the lack of reactive power supply. Furthermore, the integration capacity of a wind farm is related to wind speed PDF, WTG technological parameters, and WTG investment cost. The WTG type possessing a smaller difference in characteristic wind speeds corresponds to the smaller wind speed disturbance, which increases the utilization efficiency and optimal average integration power of WTG. The economic benefit of a wind farm can be improved by decreasing the manufacturing cost of WTG.

In summary, only when the appropriate WTG construction scheme is chosen according to special operation conditions can the maximum economic benefit of a wind farm be acquired. The proposed optimization model in this paper can also determine the effect of influencing factors by modifying the relative constraints and known parameters based on research need.

## Acknowledgement

This work was supported by the Scientific Research Foundation of State Key Lab of Power Transmission Equipment and System Security (2007DA10512712205).

## 7 References

- [1] François, B.; Francisco, D. G. Stochastic Security for Operations Planning with Significant Wind Power Generation. // IEEE Trans. Power Syst. 23, 2(2008), pp. 306-316.
- [2] Jianhui, W.; Mohammad, S.; Zuyi, L. Security-Constrained Unit Commitment with Volatile Wind Power Generation. // IEEE Trans. Power Syst. 23, 3(2008), pp. 1319-1327.

- [3] Karki, R.; Billinton, R. Cost-effective Wind Energy Utilization for Reliable Power Supply. // IEEE Trans. Energy Convers. 19, 2(2004), pp. 435-440.
- [4] Billinton, R.; Bai, G. Generating Capacity Adequacy Associated with Wind Energy. // IEEE Trans. Energy Convers. 19, 3(2004), pp. 641-646.
- [5] Sørensen, J. D. Optimal, Reliability-based Turbine Placement in Offshore Wind Turbine Parks. // Civil Eng. Environ. Syst. 24, 2(2007), pp. 99-109.
- [6] Billinton, R.; Gao, Y. Multistate Wind Energy Conversion System Models for Adequacy Assessment of Generating Systems Incorporating Wind Energy. // IEEE Trans. Energy Convers. 23, 1(2008), pp. 163-170.
- [7] Luo, C.; Far, H. G.; Banakar, H. Estimation of Wind Penetration as Limited by Frequency Deviation. // IEEE Trans. Energy Convers. 22, 3(2007), pp. 783-791.
- [8] Eknath, V.; McCalley, J. D.; Ajjarapu, V. Wind Penetration Limited by Thermal Constraints and Frequency Stability. // In Proceedings of 39<sup>th</sup> North American Power Symposium: Power Engineering Society / Las Cruces, USA, 2007, pp. 353-359.
- [9] Yazhou, L.; Weisheng, W.; Yonghua, Y. Optimal Real Power Flow in Wind Power Integrated System. // Power System Technology. 26, 6(2002), pp. 18-21.
- [10] Baogong, S.; Peng, Y.; Guanghui, S. Wind Power Penetration Limit Assessment based on Nonlinear Interior Point Algorithm. // Proceedings of the CSEE. 30, 10(2010), pp. 23-28.
- [11] Yazhou, L.; Weisheng, W.; Yonghua, Y. An Optimization Method for Determining Wind Power Penetration Limit in Power System under Static Security Constraints. // Proceedings of the CSEE. 21, 6(2001), pp. 25-28.
- [12] Guoqiang, Z.; Hai, B.; Shuyong, C. Amending Algorithm for Wind Farm Penetration Optimization based on Approximate Linear Programming Method. // Proceedings of the CSEE. 24, 10(2004), pp. 68-71.
- [13] Jun, W.; Guojie, L.; Yuanzhang, S. Maximum Injection Power Calculation of Wind Farms Connected to Power Systems based on Probabilistically Programming. // Power System Technology. 31, 14(2007), pp. 15-19.
- [14] Yazhou, L.; Weisheng, W.; Yonghua, Y. Wind Power Penetration Limit Calculation based on Chance Constrained Programming. // Proceedings of the CSEE. 22, 5(2002), pp. 32-35.
- [15] Jiageng, Q.; Fei, X.; Zongxiang, L. Optimization Analysis Model of Grid-connected Wind Capacity based on Dependent Chance Programming. // Automation of Electric Power Systems. 32, 10(2008), pp. 84-87.
- [16] Rui, W.; Wei, G.; Rong, S. Analysis on Wind Power Penetration Limit based on Probabilistically Optimal Power Flow. // Power System Technology. 35, 12(2011), pp. 214-220.
- [17] Si, L.; Renjun, Z.; Xiaojiao, T. Robust Optimization with Box Set for Maximum Installed Capacity of Wind Farm Connected to Grid. // Power System Technology. 35, 12(2011), pp. 208-213.
- [18] Denny, E.; Malley, O. A Quantitative Analysis of the Net Benefits of Grid Integrated Wind. // In Proceeding of IEEE Power Engineering Society General Meeting / Montreal, Canada, 2006, pp. 5-10.
- [19] Kaigui, X.; Billinton, R. Determination of the Optimum Capacity and Type of Wind Turbine Generators in a Power System Considering Reliability and Cost. // IEEE Trans. Energy Convers. 26, 1(2011), pp. 227-234.
- [20] Vandad, H. L.; Furong, L. Value of Wind Power at Different Locations in the Grid. // IEEE Trans. Power Deliv. 26, 2(2011), pp. 526-537.
- [21] Ha, T.; Surya, S. Augmenting Wind Power Penetration and Grid Voltage Stability Limits Using ESS: Application Design, Sizing, and a Case Study. // IEEE Trans. Power Syst., 27, 1(2012), pp. 161-171.
- [22] Billinton, R.; Chen, H. Determination of the Optimum Site-matching Wind Turbine Using Risk-based Capacity Benefit Factors. // IEE Proc-Gener. Transm. Distrib., 146, 1(1999), pp. 96-100.
- [23] Renewable Energy Law of People's Republic of China. People's Republic of China: Beijing, P. R. China, 2005, pp. 1-30.
- [24] Masters, G. Renewable and efficient electric power systems. Wiley-IEEE Press, Hoboken, NJ, USA, 2004.
- [25] Grove-Kuska, N.; Heitsch, H.; Romisch, W. Scenario Reduction and Scenario Tree Construction for Power Management Problems. // In Proceeding of IEEE Bologna Power Technology Conference / Bologna, Italy, 2003.
- [26] Zhihua, C. Social Emotional Optimization Algorithm. Publishing House of Electronics Industry, Beijing, P. R. China, 2011.
- [27] Yongqi, D. The Development of FRP Blade about Wind Turbine Generator in Worldwide Area. // Fiber Composites, 3(2001), pp. 46-49.
- [28] Zhen, J.; Huilian, L.; Qinghua, W. Particle Swarm Optimization Algorithm and its Application. Science Press, Beijing, P. R. China, 2009.

#### Authors' addresses

##### **Yingzhao Xie, Dr. in Electrical Engineering**

State Key Laboratory of Power Transmission Equipment & System Security and New Technology (Chongqing University)  
Room 6103, School of Electrical Engineering (the 6th Teaching Building)  
Campus A, Chongqing University,  
No. 174 Sha zhengjie, Sha pingba District,  
400044 Chongqing, P. R. China  
E-mail: xie\_ying\_zhao@163.com

##### **Jiping Lu, Prof. in Electrical Engineering**

State Key Laboratory of Power Transmission Equipment & System Security and New Technology (Chongqing University)  
Room 6103, School of Electrical Engineering (the 6th Teaching Building)  
Campus A, Chongqing University,  
No. 174 Sha zhengjie, Sha pingba District,  
400044 Chongqing, P. R. China  
E-mail: lujiaping@cqu.edu.cn